



**NJC**

**Amplification of Impurity upon Complex Formation: How a  
2% Ligand Impurity Lowers the Corresponding Complex  
Purity to 50%**

Journal:	<i>New Journal of Chemistry</i>
Manuscript ID	NJ-LET-08-2018-004176.R1
Article Type:	Paper
Date Submitted by the Author:	27-Sep-2018
Complete List of Authors:	Liyana Gunawardana, Vageesha ; Western Michigan University Mezei, Gellert; Western Michigan University, Chemistry

SCHOLARONE™  
Manuscripts

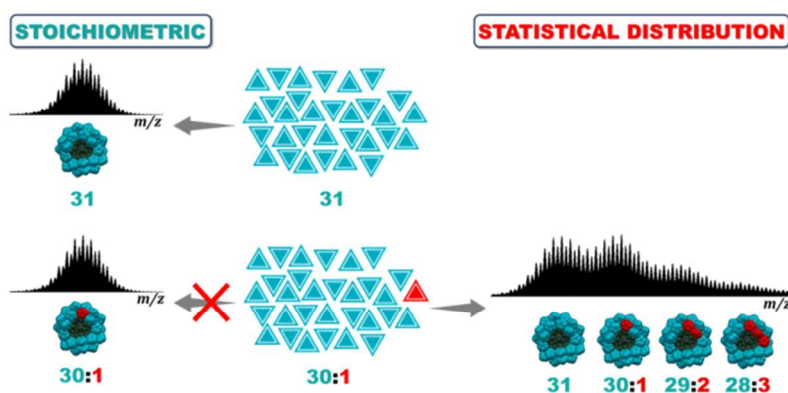
# Amplification of Impurity upon Complex Formation: How a 2% Ligand Impurity Lowers the Corresponding Complex Purity to 50%†

Vageesha W. Liyana Gunawardana and Gellert Mezei\*

*Department of Chemistry, Western Michigan University, Kalamazoo, Michigan, USA*

## ABSTRACT

Small amounts of an impurity in a ligand can be greatly amplified upon formation of large metal-organic complexes, exemplified here by the formation of alkyne-functionalized nanojars. We demonstrate that the incorporation of the pyrazole ligand impurity into the nanojar is governed by statistics and does not directly reflect the actual ratio between the ligand and the impurity.



## 1. Introduction

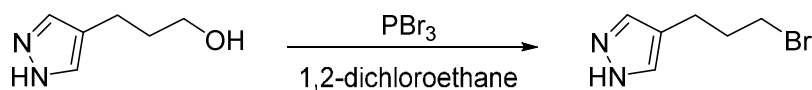
Purity is often a crucial aspect of chemicals, as even a trace amount of an impurity can drastically change their properties and render them useless for certain applications. For example, a mere 0.0001% impurity (such as 1 B atom per 1,000,000 Si atoms) increases the conductivity of silicon by a factor of  $\sim 10^6$ .<sup>1</sup> Purification of metallurgical grade Si (98%) to semiconductor grade Si (>99.9999999%) requires sophisticated, energy-intensive processes which increase the price of the final product by orders of magnitude. Purity is also critical in the pharmaceutical industry, where identification of impurities above 0.05% is often needed.<sup>2</sup> In general, however, high purity does not warrant the cost of purification processes, typically accompanied by the generation of large amounts of waste, and the elaborate analytical techniques required for quantification. Reagent-grade chemicals, for instance, are typically sold as 98–99% pure. Also, 1–3% impurities in a final product are generally acceptable during routine organic synthesis. Herein we reveal that, in stark contrast with standard practices, allowing a mere 2% impurity in a ligand lowers the purity of the corresponding metal complex derivative to  $\sim 50\%$ .

Nanojars are large metal-organic complexes comprised of 26–36 repeating units of  $[\text{Cu}(\mu\text{-OH})(\mu\text{-pz})]$  (pz = pyrazolato anion), which strongly and selectively incarcerate highly hydrophilic oxoanions.<sup>3</sup> Aiming at preparing nanojars equipped with reactive groups that would allow for derivatization by various functionalities, we selected the ‘click reaction’ (alkyne-azide cycloaddition)<sup>4</sup> as a possible post-synthetic nanojar functionalization methodology. Crucial for the suitability of such strategy is that the reactive groups on the nanojar periphery and the functional moiety to be attached, as well as the coupling reaction conditions, do not interfere with the structure of the nanojar. We have shown previously that functional groups such as phenol, thiol, amine, aldehyde, carboxylic acid or other groups more acidic than water are not compatible with nanojars.<sup>3a,f</sup> Therefore, we chose to prepare alkyne-functionalized nanojars, from which derivatives could be obtained by reaction with various azide-functionalized moieties (such as a fluorescent label). The ‘click reaction’ can conveniently be performed at room temperature if catalyzed by Cu(I) salts, and generally provides excellent yields.

## 2. Experimental section

### 2.1. General methods

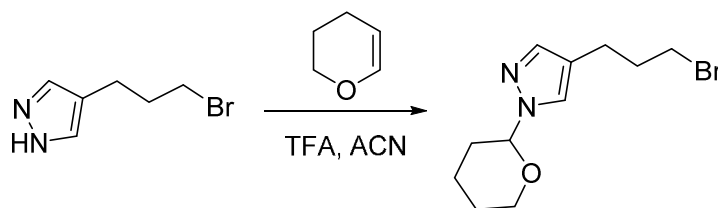
THF was dried using sodium/benzophenone ketyl. All other reagents were used as received. Standard Schlenk line techniques were used for air- and moisture-sensitive reactions. Mass spectrometry was performed on a Waters Synapt G1 HDMS instrument with electrospray ionization (ESI). The electrospray capillary voltage was set to 2.5 kV with desolvation temperature of 85 °C. Sampling and extraction cones were set at 40 V and 1.0 V, respectively. The source temperature was 80 °C with nebulizing gas supplied at 250 L/h. Samples were infused at 10–25  $\mu\text{L}/\text{min}$ .  $^1\text{H}$  and  $^{13}\text{C}$  NMR spectra were collected using a Jeol 400 MHz instrument.



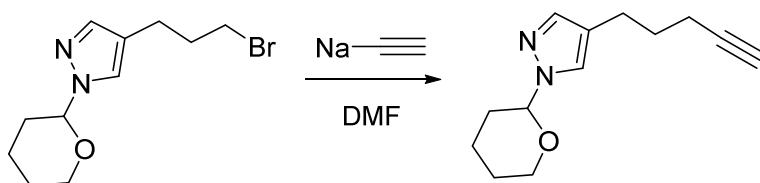
### 2.2. Ligand synthesis

**4-(3-bromopropyl)pyrazole (2).** In a 250 mL 3-necked round bottom flask equipped with a jacketed and pressure equalizing addition funnel, 4-(3-hydroxypropyl)pyrazole (13.0 g, 103 mmol) was slurried in 1,2-dichloroethane (150 mL). The flask was purged with  $\text{N}_2$  and cooled in an ice bath. Phosphorus tribromide (30.0 mL, 85.5 g, 316 mmol) was added dropwise from the addition funnel to the reaction mixture under stirring, over 40 mins. The resulting mixture was allowed to stir in the ice bath for 30 mins. Then, the addition funnel was replaced by a condenser equipped with a drying tube (containing anhydrous  $\text{CaCl}_2$ ) and the reaction mixture was refluxed for 3h. After cooling down overnight, the reaction mixture was placed in an ice bath and was quenched carefully with solid  $\text{NaHCO}_3$  (effervescence) until  $\text{pH} \approx 8$  (~75 g). Water (200 mL) was added in small portions, and the aqueous layer was extracted with dichloromethane (250 mL  $\times$  4) in a separatory funnel. The combined organic layers were washed with water (400 mL  $\times$  4) and brine (400 mL), and dried over anhydrous  $\text{MgSO}_4$ . After filtration, the solvent was removed under reduced pressure affording 13.7 g (71%) of **2** as a white crystalline solid.  $^1\text{H}$  NMR (400 MHz,  $\text{CDCl}_3$ ):  $\delta$  7.44 (s, 2H, 3,5-*H*-pz), 3.40 (t, 2H,  $\text{CH}_2\text{Br}$ ,  $J = 7$  Hz), 2.68 (t, 2H, pz $\text{CH}_2$ ,  $J = 7$  Hz), 2.10 (m, 2H,  $\text{CH}_2\text{CH}_2\text{CH}_2$ ) ppm.  $^{13}\text{C}$  NMR (400 MHz,  $\text{CDCl}_3$ ):  $\delta$  132.9, 119.1, 33.7, 33.2, 22.3 ppm.

HRMS (ESI-TOF)  $m/z$ :  $[M + H]^+$  calcd. for  $C_6H_{10}BrN_2$  189.0027; found 188.9998. Compound **2** turns into an orange-yellow oil if kept at room temperature and NMR indicates decomposition; it did not change, however, on storage at  $-10\text{ }^\circ\text{C}$  after 1 year.



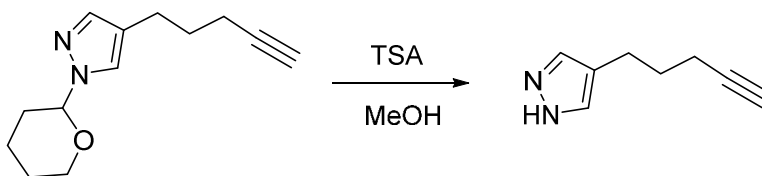
**4-(3-bromopropyl)-1-(tetrahydropyran-2-yl)pyrazole (3).** 4-(3-bromopropyl)pyrazole (10.6 g, 56.1 mmol), acetonitrile (30 mL), 3,4-dihydro-2H-pyran (5.60 mL, 5.16 g, 61.4 mmol) and trifluoroacetic acid (0.430 mL, 0.641 g, 5.61 mmol) were combined in a 100 mL round bottom flask and the mixture was refluxed under stirring for 7 hours. After cooling overnight, it was quenched with saturated  $\text{NaHCO}_3$  solution until  $\text{pH} \approx 8$ . The resulting mixture was extracted with dichloromethane (30 mL  $\times$  2), and the combined organic layers were dried over anhydrous  $\text{MgSO}_4$ . After filtration, the solvent was removed under reduced pressure yielding 15.2 g (99%) of **3** as an orange oil.  $^1\text{H}$  NMR (400 MHz,  $\text{CDCl}_3$ ):  $\delta$  7.42 (s, 1H, 3-*H*-pz), 7.39 (s, 1H, 5-*H*-pz), 5.31 (dd, 1H, *CH*-THP), 4.05 (m, 1H, *CH*<sub>2</sub>O-THP), 3.68 (td, 1H, *CH*<sub>2</sub>O-THP), 3.40 (t, 2H, *CH*<sub>2</sub>Br,  $J = 7$  Hz), 2.63 (t, 2H, pz*CH*<sub>2</sub>,  $J = 7$  Hz), 1.99–2.19 (m, 5H, *CH*<sub>2</sub>*CH*<sub>2</sub>*CH*<sub>2</sub>, *CH*<sub>2</sub>-THP), 1.47–1.87 (m, 3H, *CH*<sub>2</sub>-THP) ppm.  $^{13}\text{C}$  NMR (400 MHz,  $\text{CDCl}_3$ ):  $\delta$  139.2, 126.2, 120.2, 87.7, 68.0, 33.5, 33.2, 30.6, 25.0, 22.6, 22.5 ppm. HRMS (ESI-TOF)  $m/z$ :  $[M + \text{Na}]^+$  calcd. for  $C_{11}H_{17}BrN_2\text{NaO}$  295.0422; found 295.0414.



**4-(pent-4-yn-1-yl)-1-(tetrahydropyran-2-yl)pyrazole (4).** In a 500 mL 3-necked round bottom flask under  $\text{N}_2$  atmosphere, **3** (8.00 g, 29.3 mmol) was dissolved in anhydrous DMF (45 mL). The reaction flask was cooled in an ice bath and sodium acetylide (18% wt slurry in xylenes, 14.0 mL, 12.3 g, 43.9 mmol) was added slowly over 10 mins, then the

mixture was allowed to warm to room temperature. After stirring overnight, NMR showed about ~3% starting material remaining. Sodium acetylide (18% wt. slurry in xylenes, 9.2 mL, 8.19 g, 30.1 mmol) was added to drive the reaction to completion. After stirring overnight, the flask was cooled in an ice bath and carefully quenched with saturated  $\text{NH}_4\text{Cl}$  solution (~100 mL). The resulting mixture was extracted with dichloromethane (150 mL  $\times$  3) and the combined organic layers were washed with water (400 mL  $\times$  2) and brine (400 mL), and dried over anhydrous  $\text{MgSO}_4$ . After filtration and removal of the solvent under reduced pressure, the resulting brown oil was purified by column chromatography on silica gel (600 g) using 2:1 hexanes:ethyl acetate as eluent ( $R_f = 0.38$ ). Impure fractions were purified again by column chromatography on silica gel (180 g) using 2:1 hexanes:ethyl acetate as eluent giving a combined yield of 2.81 g (44%) of **4** as a colorless oil.  $^1\text{H}$  NMR (400 MHz,  $\text{CDCl}_3$ ):  $\delta$  7.40 (s, 1H, 3-*H*-pz), 7.38 (s, 1H, 3-*H*-pz), 5.31 (dd, 1H, CH-THP), 4.05 (m, 1H,  $\text{CH}_2\text{O}$ -THP), 3.68 (td, 1H,  $\text{CH}_2\text{O}$ -THP), 2.58 (t, 2H, pz $\text{CH}_2$ ,  $J = 7$  Hz), 2.20 (td, 2H,  $\text{CH}_2\text{CH}_2\text{C}$ ,  $J = 7$  Hz), 1.99–2.16 (m, 3H,  $\text{CH}_2$ -THP), 1.96 (t, 1H, CCH), 1.76 (m, 2H,  $\text{CH}_2\text{CH}_2\text{CH}_2$ ), 1.54–1.71 (m, 3H,  $\text{CH}_2$ -THP) ppm.  $^{13}\text{C}$  NMR (400 MHz,  $\text{CDCl}_3$ ):  $\delta$  139.5, 125.9, 121.1, 87.7, 84.2, 68.7, 67.9, 30.5, 29.5, 25.1, 23.1, 22.7, 17.9 ppm. HRMS (ESI-TOF)  $m/z$ :  $[\text{M} + \text{Na}]^+$  calcd. for  $\text{C}_{13}\text{H}_{18}\text{N}_2\text{NaO}$  241.1317; found 241.1345.

The procedure described above yields pure **4**; if purification is carried out by distillation instead of column chromatography, the product retains some of the dehydrobromination product, 4-(prop-2-en-1-yl)-1-(tetrahydropyran-2-yl)pyrazole, which will lead to ~2% 4-(prop-2-en-1-yl)pyrazole (**6**) impurity in ligand **5** upon deprotection (described in the next step).



**4-(pent-4-yn-1-yl)pyrazole (5).** Compound **4** (139 mg, 0.637 mmol) and *p*-toluenesulfonic acid (242 mg, 1.27 mmol) were stirred in methanol (10 mL) for 24 h at room temperature. The reaction was quenched with saturated  $\text{NaHCO}_3$  solution (30 mL) and extracted with dichloromethane (30 mL  $\times$  3). The combined organic layers were dried

with anhydrous  $\text{Na}_2\text{SO}_4$  and the solvent was removed under reduced pressure. Heating of the resulting clear oil under high vacuum (0.50 mmHg) at 85 °C for 1h resulted in the crystallization of the product on the cooler upper part of the flask. The yellow oily residue remaining at the bottom of the flask was rinsed off with methanol, and the crystals of **5** were again subjected to high vacuum to remove any residual methanol. 664 mg (78%) of pure **5** was obtained as white needle-like crystals.  $^1\text{H}$  NMR (400 MHz,  $\text{CDCl}_3$ ):  $\delta$  7.42 (s, 2H, 3,5-*H*-pz), 2.63 (t, 2H, C pz- $\text{CH}_2$ ,  $J = 7$  Hz), 2.21 (td, 2H,  $\text{CH}_2\text{CH}_2\text{C}$ ,  $J = 3, 7$  Hz), 1.98 (t, 1H, CCH,  $J = 3$  Hz), 1.79 (m, 2H,  $\text{CH}_2\text{CH}_2\text{CH}_2$ ) ppm.  $^{13}\text{C}$  NMR (400 MHz,  $\text{CDCl}_3$ ):  $\delta$  132.9, 120.1, 84.2, 29.6, 22.9, 17.8 ppm. HRMS (ESI-TOF)  $m/z$ :  $[\text{M} - \text{H}]^-$  calcd. for  $\text{C}_8\text{H}_9\text{N}_2$  133.0766; found 133.0787.

### 2.3. Nanojar synthesis

**Synthesis of  $\text{Na}_2[\text{CO}_3\text{C}\{\text{Cu}(\text{OH})(\text{HCC}(\text{CH}_2)_3\text{pz})\}_n]$  ( $n = 27, 29, 30, 31$ ).** 4-(Pent-4-yn-1-yl)pyrazole **5** (63.0 mg, 0.470 mmol),  $\text{Cu}(\text{NO}_3)_2 \cdot 2.5\text{H}_2\text{O}$  (110 mg, 0.473 mmol, 1.0 eq.), NaOH (39.6 mg, 0.990 mmol, 2.1 eq.) and  $\text{Na}_2\text{CO}_3 \cdot \text{H}_2\text{O}$  (58.8 mg, 0.474, 1.0 eq.) were stirred in THF (10 mL) for 3 days. The resulting deep blue solution was filtered, and the solvent was removed under reduced pressure. The solid was re-dissolved in THF (5 mL), followed by filtration to remove any residual insoluble material and solvent removal under reduced pressure to give 0.11 g of blue solid (100% yield based on  $\text{Cu}_{29}$  nanojar).

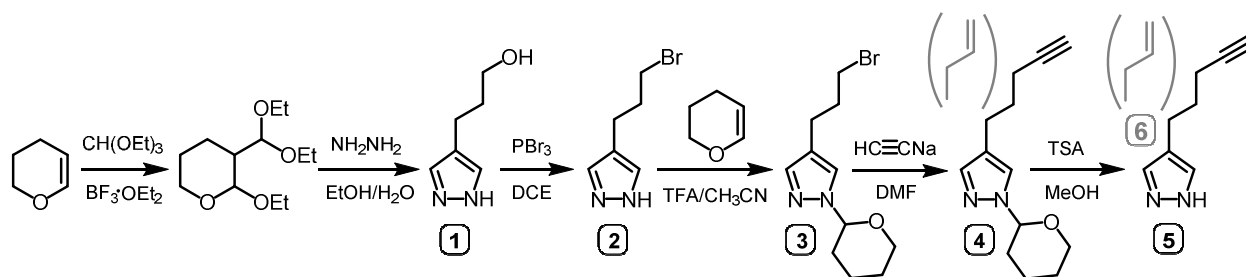
**Synthesis of  $[\text{Cu}_n(\text{OH})_n(\text{C}_3\text{H}_3\text{N}_2)_{n-x}(\text{C}_4\text{H}_5\text{N}_2)_x\text{CO}_3]^{2-}$  nanojars with varying ratios of pyrazole and 4-methylpyrazole.** Stock solutions of pyrazole (pzH;  $1.81 \times 10^{-1}$  M), 4-methylpyrazole (MepzH;  $3.36 \times 10^{-2}$  M), copper(II) nitrate (from  $\text{Cu}(\text{NO}_3)_2 \cdot 2.5\text{H}_2\text{O}$ ;  $3.48 \times 10^{-1}$  M) and  $\text{Bu}_4\text{NOH}$  (1.05 M) were prepared in THF. Reactions were carried out in 2-dram scintillation vials equipped with magnetic stir bars. First, solutions of pzH and MepzH were combined in ratios of 100:0, 99:1, 98:2, 97:3, 96:4, 95:5, 94:6, 93:7, 92:8, 91:9 and 90:10, respectively, for a total of 70.6  $\mu\text{mol}$  of ligand in each case. Table S1 summarizes the actual mole fractions of MepzH ( $j$ ) in each solution. Under rapid stirring, the copper nitrate solution was added (200  $\mu\text{L}$ , 69.6  $\mu\text{mol}$ , 1.0 eq.), followed by the  $\text{Bu}_4\text{NOH}$  solution (138  $\mu\text{L}$ , 145  $\mu\text{mol}$ , 2.05 eq.), leading to a deep-blue colored, clear solution. The  $\text{CO}_3^{2-}$  ion in the nanojars originates from the  $\text{Bu}_4\text{NOH}$  solution, which contains small amounts of carbonate.

After stirring for 5 mins, this solution was poured into H<sub>2</sub>O (~10 mL). The resulting blue precipitate was filtered out, rinsed with water and dried in air. Mass spectrometry samples were prepared by dissolving the complete amount obtained from the reactions in mass spectrometry grade acetonitrile (25.0 mL, 97 mM assuming quantitative yield).

<i>[pz:4-Mepz]</i>	<i>j</i>
<i>[100:0]</i>	0
<i>[99:1]</i>	0.0096
<i>[98:2]</i>	0.0192
<i>[97:3]</i>	0.0289
<i>[96:4]</i>	0.0385
<i>[95:5]</i>	0.0482
<i>[94:6]</i>	0.0577
<i>[93:7]</i>	0.0674
<i>[92:8]</i>	0.0771
<i>[91:9]</i>	0.0867
<i>[90:10]</i>	0.0964

### 3. Results and discussion

To synthesize the terminal alkyne-functionalized pyrazole ligand, 4-(3-hydroxypropyl)pyrazole (**1**) was prepared first,<sup>5</sup> which was subsequently converted to 4-(3-bromopropyl)pyrazole (**2**) by reaction with PBr<sub>3</sub>. After protecting the pyrazole ring with a tetrahydropyran-2-yl (THP) group, the terminal bromo functionality of 4-(3-bromopropyl)-1-(tetrahydropyran-2-yl)pyrazole (**3**) was reacted with sodium acetylide. Deprotection of the resulting 4-(pent-4-yn-1-yl)-1-(tetrahydropyran-2-yl)pyrazole (**4**) with methanolic *p*-toluenesulfonic acid afforded 4-(pent-4-yn-1-yl)pyrazole (**5**) in 16% overall yield after six steps, based on 3,4-dihydro-2*H*-pyran (Scheme 1).



**Scheme 1.** Synthesis of 4-(pent-4-yn-1-yl)pyrazole (**5**) from 3,4-dihydro-2*H*-pyran (DCE – dichloroethane, TFA – trifluoroacetic acid, DMF – *N,N*-dimethylformamide, TSA – toluenesulfonic acid).

Next, nanojars functionalized with alkyne moieties were targeted. The reaction of **5** ( $C_8H_{10}N_2$ ) with copper(II) nitrate and sodium hydroxide in the presence of carbonate at room temperature was expected to produce nanojars of the formula  $[CO_3\{Cu(OH)(C_8H_9N_2)\}_n]^{2-}$  ( $n = 27-31$ ). Instead, the electrospray-ionization mass spectrum (ESI-MS) of the resulting nanojar solution displayed numerous peaks in addition to the expected ones, attributable to variously substituted nanojar species containing up to four 4-(prop-2-en-1-yl)pyrazolate ( $C_6H_7N_2$ ) moieties, with the general formula  $[Cu_n(OH)_n(C_8H_9N_2)_{n-x}(C_6H_7N_2)_xCO_3]^{2-}$  ( $n = 27$ :  $x = 0$ ,  $m/z$  2915;  $x = 1$ ,  $m/z$  2902;  $x = 2$ ,  $m/z$  2889;  $n = 29$ :  $x = 0$ ,  $m/z$  3129;  $x = 1$ ,  $m/z$  3116;  $x = 2$ ,  $m/z$  3103;  $x = 3$ ,  $m/z$  3090;  $x = 4$ ,  $m/z$  3077;  $n = 31$ :  $x = 0$ ,  $m/z$  3343;  $x = 1$ ,  $m/z$  3330;  $x = 2$ ,  $m/z$  3317;  $x = 3$ ,  $m/z$  3304) (Figure 1). The origin of the unexpected 4-(prop-2-en-1-yl)pyrazole ( $C_6H_8N_2$ , **6**; **Figure 1**) can be traced back to the reaction of the bromo-derivative **3** with sodium acetylide. The latter, owing to its strongly basic character, produces small amounts of alkene **6** by dehydrobromination of **3**, in addition to the major product, alkyne **4**. It becomes apparent that a small amount (2%) of **6** retained after the purification of alkyne-pyrazole **5** by distillation, although not alarming when considering the purity of the ligand itself, has a dramatic effect on the purity of the corresponding nanojars. To obtain pure nanojars, a more thorough purification of the ligand (by column chromatography) is necessary (see SI).

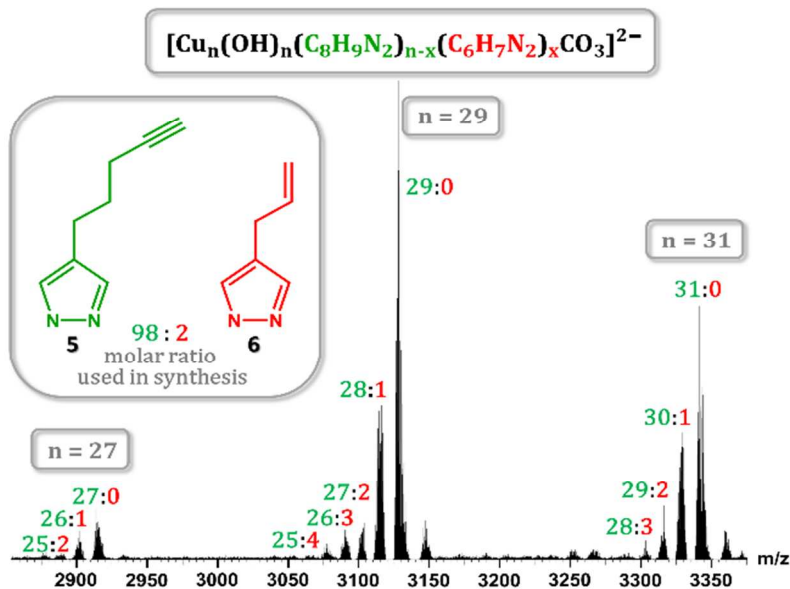


**Figure 1.** ESI-MS spectrum of the nanojar mixture obtained from 5 (with 2 mol% of 6).

To study the effect of ligand impurity on the purity of the corresponding nanojar in more depth, we carried out a rational study using mixtures of pyrazole (pzH) with varying amounts of 4-methylpyrazole (4-MepzH, 0–10 mol %). The ESI-MS spectra of the resulting nanojars, obtained by reacting the pyrazole mixture with copper nitrate and sodium hydroxide in the presence of carbonate, are shown in Figures 2, 3 and S9–S16 and lead to the following observations. In all cases, a mixture of nanojars of different sizes,  $[\text{Cu}_n(\text{OH})_n(\text{pz})_{n-x}(4\text{-Mepz})_x\text{CO}_3]^{2-}$  ( $n = 27$ , **Cu<sub>27</sub>**;  $n = 29$ , **Cu<sub>29</sub>**;  $n = 30$ , **Cu<sub>30</sub>**;  $n = 31$ , **Cu<sub>31</sub>**;  $x = 0–7$ ), is obtained. It must be noted that ESI-MS spectra do not account for possible positional isomers of the different species. Increasing amounts of 4-methylpyrazole in the ligand mixture lead to increasing amounts of Cu<sub>29</sub> and Cu<sub>30</sub> species in the resulting nanojar mixtures. Thus, in the case of the 90:10 molar mixture of pzH and 4-MepzH, the Cu<sub>30</sub> species are as abundant as the Cu<sub>27</sub> species and the Cu<sub>29</sub> species are more abundant than the Cu<sub>27</sub> species, whereas both Cu<sub>29</sub> and Cu<sub>30</sub> are minor species in the case of nanojars obtained from pure pzH. Despite the homogeneity of the ligand mixture used in the syntheses, the molar ratio of pzH:4-MepzH employed is not reflected in the number of pyrazole ligands substituted for 4-methylpyrazole in the resulting nanojar mixtures. In the case of a 97:3 molar mixture of pzH and 4-MepzH, for example, an average of approximately one 4-methylpyrazolate ligand per nanojar is expected (32:1,  $x = 1$ ). Instead,

multiply substituted species, with up to three 4-methylpyrazolates per nanojar are observed ( $x = 1-3$ ), along with non-substituted nanojars ( $x = 0$ ). In the case of the 90:10 molar mixture of pzH and 4-MepzH (27:3), which corresponds to an average  $x = 3$ , only small amounts of non-substituted nanojars are present, and substituted species with up to  $x = 7$  are observed. Thus, a 10 mol % impurity in the pyrazole ligand reduces the purity of the corresponding homoleptic nanojar to almost zero.

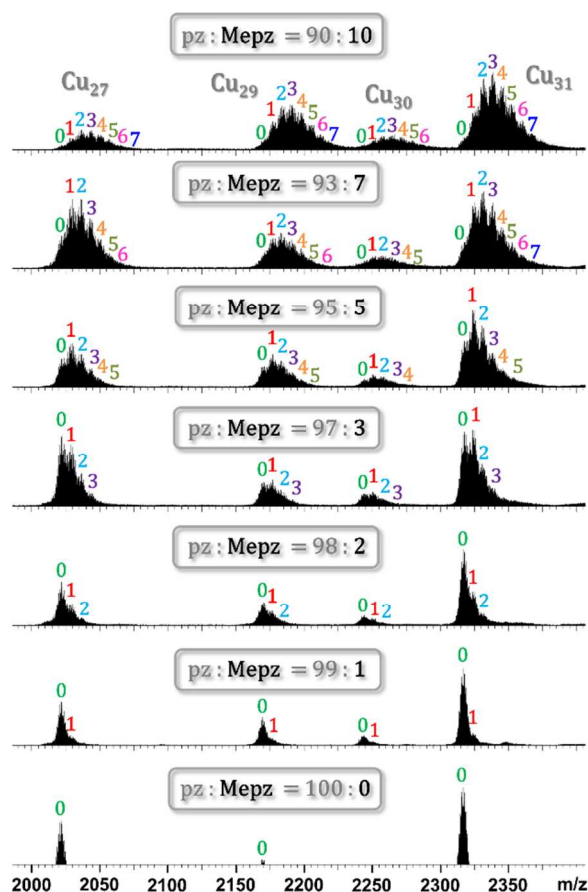


**Figure 2.** ESI-MS spectra of the nanojars obtained using pzH:4-MepzH mixtures (0–10 mol % 4-MepzH). Colored numbers indicate the number of 4-Mepz moieties per nanojar.

The distributions of nanojars containing different amounts of pz and 4-Mepz ligands, observed in Figures 2, 3 and S9–S16, suggest that the incorporation of those ligands during nanojar synthesis is governed by statistics. To test this hypothesis, we employed elementary statistical models to predict the distributions of nanojars containing different combinations of the two ligands. Similar models have been used to study the

distribution of differently substituted gold nanoparticles obtained through surface ligand exchange, and the segregation of different thiolate ligands on gold nanoparticles.<sup>6</sup>

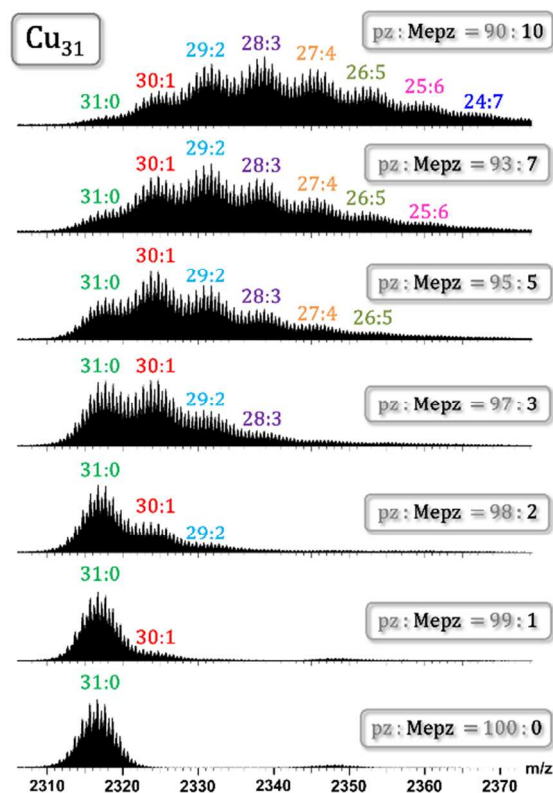
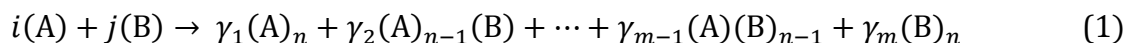


**Figure 3.** ESI-MS spectra showing the  $\text{Cu}_{31}$  nanojars obtained using pzh:4-MepzH mixtures (0–10 mol% 4-MepzH). Colored numbers indicate the ratio between pzh and 4-Mepz ligands in each species. For the analogous  $\text{Cu}_{29}$ ,  $\text{Cu}_{30}$  and  $\text{Cu}_{31}$  nanojars, see Figures S14–S16.

In statistics, the binomial distribution gives the probability ( $P$ ) of a certain event occurring  $m$  number of times in  $n$  trials, when the expectation of occurrence for any given trial is  $p$ . In terms of a binary mixture of pyrazole ligands, a generalized equation for the formation of homo- and heteroleptic  $\text{Cu}_n$  nanojars is given by:



where A and B represent pzh and 4-Mepz, respectively, and coefficients  $i$  and  $j$  indicate the employed molar ratio between the two. Each term on the right-hand side of the equation represents a possible species of nanojar, where  $n$  is the total number of ligands in the

nanojar ( $n = 27, 29, 30$  or  $31$ ). Coefficients  $\gamma_m$  indicate the relative fractions of each species ( $n \sum \gamma_m = i + j$ ). In statistical terms, each trial will lead to a nanojar species  $[\text{Cu}_n(\text{OH})_n(\text{A})_{n-x}(\text{B})_x(\text{CO}_3)]^{2-}$  with a certain number of incorporated ligands A and B. If we assume that the abundance of the different species is determined according to a binomial distribution with  $p$  representing the mole fraction  $j$  of ligand B, the following equation can be written:

$$P = \frac{n!}{x!(n-x)!} j^x (1-j)^{n-x} \quad (2)$$

The related Poisson distribution can be used as an approximation of the binomial distribution when  $n$  is large and  $p$  is small, given by the equation:

$$P = e^{-nj} \frac{(nj)^x}{x!} \quad (3)$$

The amplitudes of the peaks of each nanojar species observed in the ESI-MS spectrum were used to compare experimental results to theoretically predicted distributions. The amplitudes were converted to probabilities ( $P^*$ ) by dividing the intensity of the tallest isotopic peak of each individual nanojar by the sum of intensities of all observed species of a given size of nanojar ( $\text{Cu}_n$ ):

$$P^* = \frac{I_{n,x}}{\sum_{x=0}^n I_{n,x}} \quad (4)$$

where  $I_{n,x}$  is the intensity of the peak of nanojar of size  $n$  with  $x$  ligands B. Binomial and Poisson distributions were derived using "BINOM.DIST" and "POISSON.DIST" functions in Microsoft Excel. The differences between theoretical and experimental values were analyzed using the residual sum of squares (RSS) method.

Figure 4 shows the comparison of predicted and experimental distributions exemplified on  $\text{Cu}_{31}$  nanojars prepared using different ratios ( $i:j$ ) of pz:4-Mepz. A minute deviation of the experimental values from the theoretically predicted ones is observed; smaller ligand substitutions ( $x \leq 2$ ) are overestimated and larger substitutions ( $x > 2$ ) are underestimated by the theoretical model. This deviation is more pronounced with larger mole ratios of 4-Mepz. The distributions for different sizes of nanojars follow a similar pattern (Figures 5 and S17–S19).

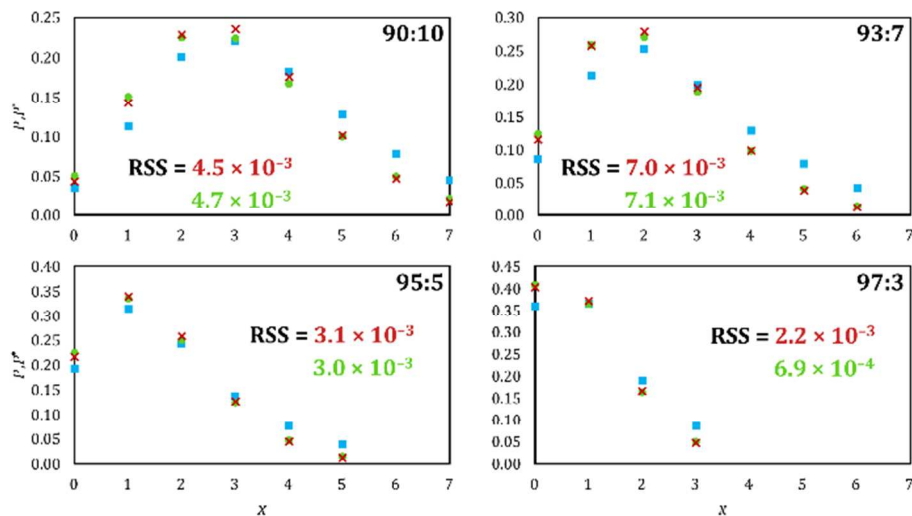


**Figure 4.** Plots of binomial (red), Poisson (green) and experimental (blue) distributions for  $\text{Cu}_{31}$  nanojars for different ratios of pz:4-Mepz.

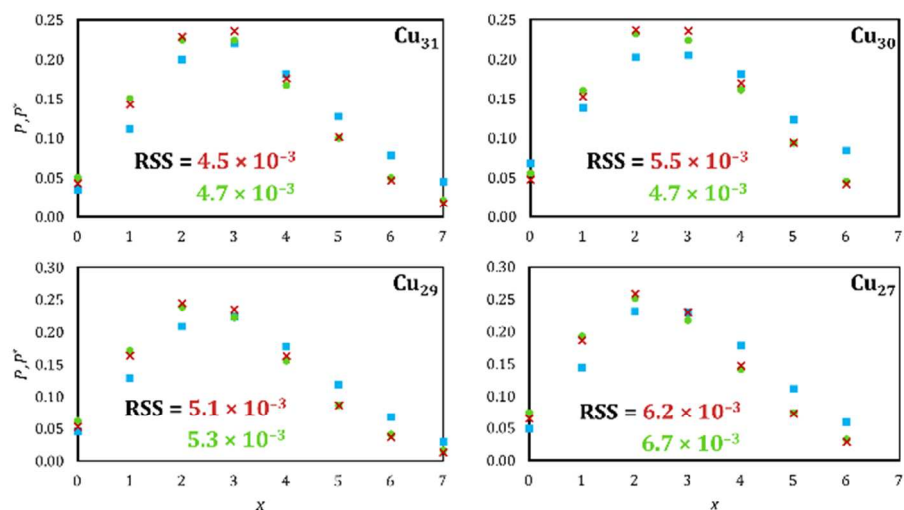


**Figure 5.** Plots of binomial (red), Poisson (green) and experimental (blue) distributions for different sized nanojars with 90:10 pz:4-Mepz ligand mixture.

The binomial and Poisson distributions can be used to fit the experimentally observed distributions by empirically deriving the value of  $j$  in equation 2 and 3 by treating the data as a frequency distribution:

$$j_{ad} = \frac{1}{n} \left( \frac{\sum_{x=0}^n I_{n,x} * x}{\sum_{x=0}^n I_{n,x}} \right) \quad (5)$$

where  $j_{ad}$  is the adjusted probability of ligand substitution per trial. Plots of experimental and theoretical distributions using  $j_{ad}$  are shown in Figures 6 and S20–S22. The lower RSS

values as compared to those of Figure 5 indicate a better fit of the theoretical values with experimental observations.

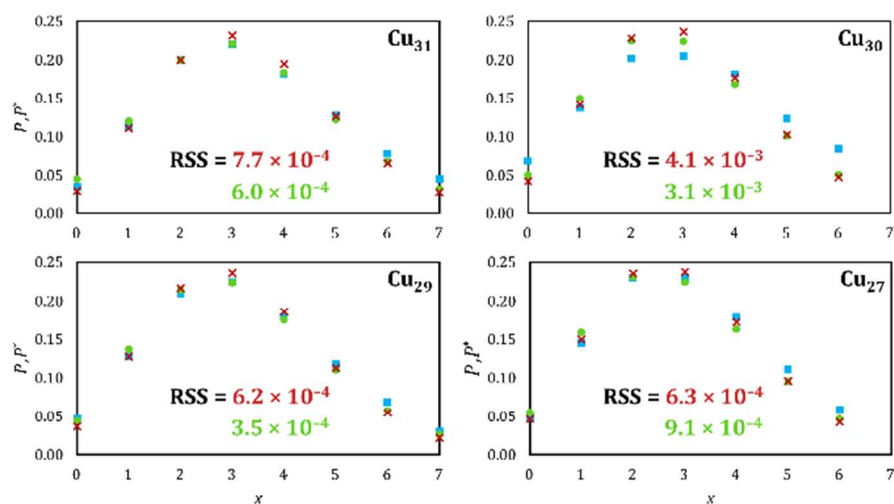


**Figure 6.** Plots of binomial (red), Poisson (green) and experimental (blue) distributions using  $j_{ad}$  for different sized nanojars with 90:10 pz:4-Mepz ligand mixture.

In a wider context, the phenomenon of impurity amplification is expected to apply to other discrete self-assembled structures as well. The effect of the amount of ligand impurities on the composition of self-assembled structures is dependent on the number of components in the assembly, as illustrated by Figure 7. As even the substitution of a single ligand in an assembly results in a distinct species, the larger the number of components, the more susceptible the assembly is to small amounts of ligand impurities with similar binding properties. Non-binding impurities will not alter the composition of the assembly, whereas large differences in binding affinity of the two ligands may result in self-sorting behavior, where assemblies containing one type of ligand will be preferred over the other.

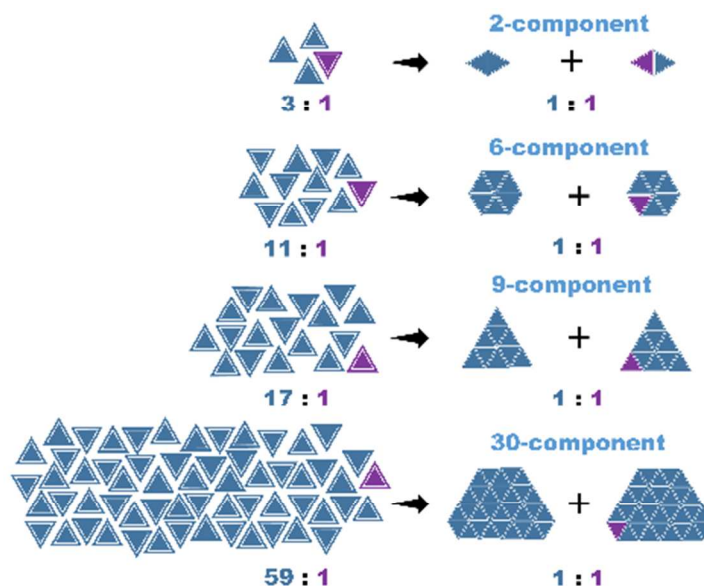


**Figure 7.** Translation of ligand impurity to impurities in self-assembled structures.

The quantitative relationship between the number of ligands in an assembly and the amount of ligand impurity can be derived by rearranging equation 2. If we are concerned about the purity of the parent assembly containing only ligand A, we can set  $x = 0$ , resulting in:  $P = (1 - j)^n$ . Raising both sides of the equation to the power of  $1/n$  and rearranging gives:

$$j = 1 - P^{\frac{1}{n}} \quad (6)$$

By setting  $P = 0.5$ , we can calculate the amount of ligand impurity required to reduce the purity of a self-assembled structure by half for a given size of assembly. A plot of equation 6 is shown in Figure 8. Assuming completely random association of ligands to form a set of binomially distributed species, this equation predicts that only 2.2 mol% of a pyrazole impurity is required to reduce the purity of a  $\text{Cu}_{31}$  nanojar by half. By using the same equation, it can be derived similarly that the ligand should contain no more than 0.10 mol% impurity with similar binding properties in order to obtain a  $\text{Cu}_{31}$  nanojar of 97 mol% purity, and no more than 0.032 mol% if a purity of 99 mol% is desired.

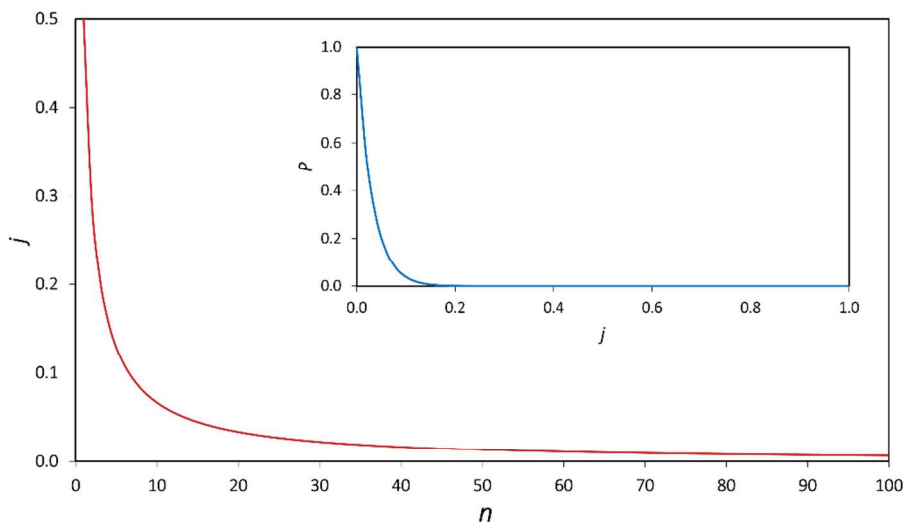


**Figure 8.** Plot of equation 6 illustrating the relationship between amount of impurity and complex size when  $P = 0.5$  ( $n$  is the number of components in the complex and  $j$  is the mole fraction of impurity). Inset: effect of amount of ligand impurity as mole fraction ( $j$ ) on the purity of a  $\text{Cu}_{31}$  nanojar, represented by  $P$ .

## 4. Conclusions

In summary, herein we addressed the preparation of functionalized nanojars amenable to post-synthetic modifications, exemplified by alkyne-decorated species which can undergo click chemistry. We demonstrated that ligand purity is crucial for the preparation of large metal-organic complexes in pure form, as even very small amounts of impurities with similar binding properties lead to drastic reduction of product purity. The severity of this effect is exacerbated by the fact that impurity incorporation is governed by statistical distribution rather than stoichiometric incorporation, leading to complex product mixtures. We have quantified the effect of the amount of ligand impurity on the purity of the corresponding complex, which is dependent on the number of constituent ligands: the more ligands, the more susceptible the complex is to small amounts of impurity. Although nanojars are unique to copper,<sup>3c</sup> metal complexes in general can also have a similar susceptibility to small amounts of metal impurities, if the different metal can form the same type of complex.

### ■ ASSOCIATED CONTENT

#### Supporting Information

The Supporting Information is available on the ACS Publications website at DOI: 10.1021/acs.jchemed.

Details of ESI-MS and NMR spectra, plots of binomial, Poisson and experimental nanojar distributions.

## ■ AUTHOR INFORMATION

### Corresponding Author

\*E-mail: gellert.mezei@wmich.edu.

### ORCID

Gellert Mezei: 0000-0002-3120-3084

Vageesha W. Liyana Gunawardana: 0000-0001-5053-4236

### Notes

† Dedicated to Professor Rodica Micu-Semeniuc on her 80<sup>th</sup> birthday

The authors declare no competing financial interest.

## ■ ACKNOWLEDGMENTS

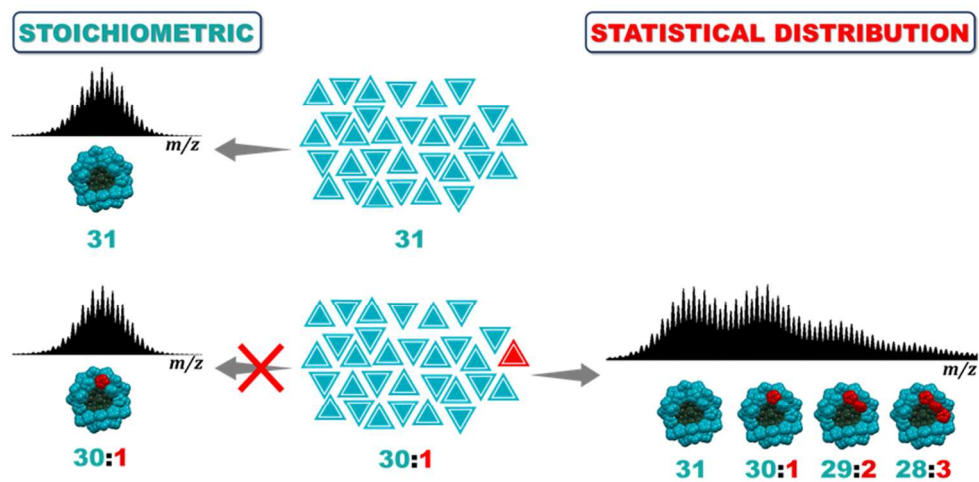
This work was funded by the National Science Foundation under Grant No. CHE-1404730.

## ■ REFERENCES

- 1 Holleman, A. F.; Wiberg, E. *Inorganic Chemistry*, Academic Press, 2001, p. 1241.
- 2 (a) ICH Q3A(R2), 2006. Impurities in new drug substances. Step 4, October 2006; (b) R. Holm and D. P. Elder, *Eur. J. Pharm. Sci.*, 2016, **87**, 118–135; (c) G. F. Pauli, S.-N. Chen, C. Simmler, D. C. Lankin, T. Gödecke, B. U. Jaki, J. B. Friesen, J. B. McAlpine and J. G. Napolitano, *J. Med. Chem.*, 2014, **57**, 9220–9231; (d) H. A. Moynihan and D. E. Horgan, *Org. Process Res. Dev.*, 2017, **21**, 689–704.
- 3 (a) B. M. Ahmed and G. Mezei, *Chem. Commun.*, 2017, **56**, 1029–1032; (b) C. K. Hartman, G. Mezei, *Inorg. Chem.*, 2017, **56**, 10609–10624; (c) W. A. Al Isawi, B. M. Ahmed, C. K. Hartman, A. N. Seybold and G. Mezei, *Inorg. Chim. Acta.*, 2018, **475**, 65–72; (d) B. M. Ahmed, B. R. Szymczyna, S. Jianrattanasawat, S. A. Surmann and G. Mezei, *Chem. Eur. J.*, 2016, **22**, 5499–5503; (e) B. M. Ahmed, B. Calco and G. Mezei, *Dalton Trans.*, 2016, **45**, 8327–8339; (f) B. M. Ahmed and G. Mezei, *Inorg. Chem.*, 2016, **55**, 7717–7728; (g) B. M.

- Ahmed, C. K. Hartman and G. Mezei, *Inorg. Chem.*, 2016, **55**, 10666–10679; (h) G. Mezei, *Chem. Commun.*, 2015, **51**, 10341–10344; (i) I. R. Fernando, S. A. Surmann, A. A. Urech, A. M. Poulsen and G. Mezei, *Chem. Commun.*, 2012, **48**, 6860–6862; (j) G. Mezei, P. Baran and R. G. Raptis, *Angew. Chem. Int. Ed.*, 2004, **43**, 573–577.
- 4 (a) H. C. Kolb, M. G. Finn and K. B. Sharpless, *Angew. Chem. Int. Ed.*, 2001, **40**, 2004–2021; (b) L. Liang and D. Astruc, *Coord. Chem. Rev.*, 2011, **255**, 2933–2945.
- 5 R. G. Jones and M. J. Mann, *J. Am. Chem. Soc.*, 1953, **75**, 4048–4052.
- 6 (a) A. Dass, K. Holt, J. F. Parker, S. W. Feldberg and R. W. Murray, *J. Phys. Chem. C.*, 2008, **112**, 20276–20283; (b) K. M. Harkness, A. Balinski, J. A. McLean, D. E. Cliffel, *Angew. Chem. Int. Ed.*, 2011, **50**, 10554–10559.

Statistical incorporation of small amounts of ligand impurities has devastating consequences on the purity of metal-organic complexes derived from the respective ligands.



Graphic for TOC

80x39mm (300 x 300 DPI)